Solid State Ionics 9 & 10 (1983) 539-542
North-Holland Publishing Company

FLUORINE MOBILITY IN $La_{1-x}Ba_xF_{3-x}$ ($0 < x < 0.1$) STUDIED BY NUCLEAR MAGNETIC RESONANCE

A.F. Aalders, A. Folman, A.F.M. Arts and H.W. de Wijn

Fysisch Laboratorium, Rijksuniversiteit Utrecht
P.O. Box 80.000, 3508 TA Utrecht, The Netherlands

The fluorine mobilities in pure LaF_3 and LaF_3 doped with up to 10 mole % Ba have been studied by observing the ^{19}F NMR relaxation times T_2 and $T_{1\rho}$ versus temperature in the range 200 to 1050 K.
The data are consistent with a model of two fluorine sublattices with distinct correlation times and coupled by exchange.
The distinction becomes less apparent with concentration.
T_1 appears to be dominated by relaxation associated with the impurities and dopant ions.

1. INTRODUCTION

Many experimental studies have been devoted to the fluorine motion in the solid electrolyte LaF_3 [1-7]. The detailed interpretation of the results is however still fragmentary, mainly because of the intricate crystal structure. In the LaF_3 structure ($P\bar{3}c1$) the fluorine ions are situated on three inequivalent positions [8]. As far as the mobilities are concerned, two of these turn out to be equivalent, leaving two distinct fluorine sublattices, as was first demonstrated by Goldman and Shen [2]. The sublattices have occupancies in the ratio 2:1, and are denoted below by F_1 and F_2, respectively (Fig.1).

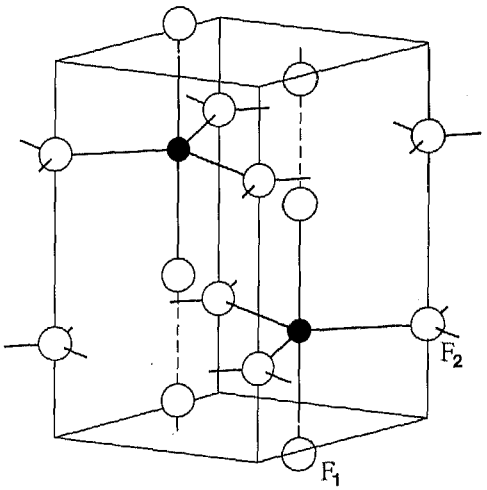

Figure 1 : Simplified structure of LaF_3.

Above room temperature the mobility on the F_2 sublattice is larger than on the F_1 sublattice.

A very suitable technique to unravel the fluorine hopping within the sublattices, as well as the hopping between them, is ^{19}F NMR. Indeed, by measurement of T_2, exchange of fluorine between the F_1 and F_2 positions has become manifest at high temperatures ($T > 400$ K for pure LaF_3) [2]. This is confirmed by the results of measurements of $T_{1\rho}$ below. We further have performed NMR relaxation time measurements of T_2, $T_{1\rho}$, and T_1 in LaF_3 doped with Ba. Here,advantage is taken of the vacancies introduced into the lattice by a divalent (in contrast to ref. [2] nonparamagnetic) dopant, which allow external control of the fluorine motion. For up to 11 mole % of Ba^{2+} $La_{1-x}Ba_xF_{3-x}$ maintains the LaF_3 structure [9].

2. EXPERIMENTAL

The crystals were prepared by the method described by Roos [10]. For NMR at room temperature and above, the crystals were sealed in a quartz ampule under a noble gas atmosphere, which resulted in excellent reproducibility against thermal cycling, even for temperatures above 1000 K. The coil was mounted externally on the ampule. For the measurements below room temperature the coil was wound directly around the crystal, permitting a better filling of the coil. Pulse sequences suitable for measurement of T_2, $T_{1\rho}$, and T_1 were generated with an M 6800 microcomputer system. The decay and spin-echo signals were stored in a Biomation 8100 fast digitizer, and fed to the microcomputer for efficient signal averaging and data reduction. The spin-spin relaxation times T_2 were obtained from the free induction decay following a 90° pulse. For long times, however, spin-echo techniques were used to avoid the effects of the magnetic-field inhomogeneities. In addition to pure LaF_3, the relaxation times were measured for Ba concentrations of 0.3, 0.9, 5, and 10 mole %.

3. RESULTS

3.1 Spin-spin relaxation

We first present the results for T_2. In the temperature range where the exchange of ions between the F_1 and F_2 sublattices is slow, the

0 167-2738/83/0000--0000/$ 03.00

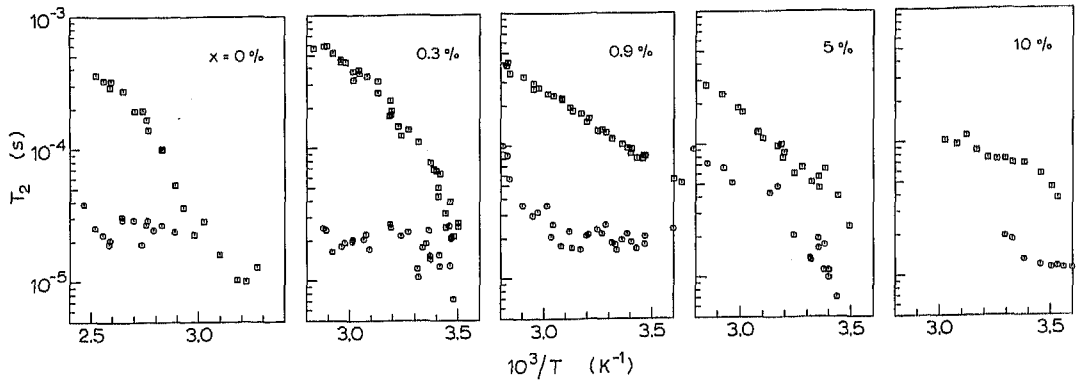

Figure 2 : Spin-spin relaxation times T_2 in $La_{1-x}Ba_xF_{3-x}$ for x = 0, 0.3, 0.9, 5, and 10 mole %, respectively. ⊡ refers to the F_2 sublattice, ⊙ to the F_1 sublattice. The F_1 sublattice is rigid in the temperature regime where T_2 associated with F_1 is constant.

free-induction decays are composite due to the different mobilities on the two sublattices. In all samples (Fig. 2), fitting the decays in this range to a sum of two exponentials yielded good results. In pure LaF_3 the fast decay exhibited a small oscillation, which was neglected in the fits. The slow decay time can be determined more accurately than the fast one. The intensities of the fast and slow decays, when extrapolated back to zero time, are in the ratio close to 2:1. This unambiguously establishes the faster motion to take place on the F_2 sublattice.

From inspection of Fig.2 it can be seen that upon Ba doping the onset of the motional narrowing shifts on both sublattices towards lower temperatures. However, for Ba concentrations up to 1 mole % there remains a regime of temperatures, varying with the concentration, where T_2 associated with F_1 is a constant, thus indicating that the F_1 sublattice is still rigid. Beyond Ba concentrations of, say, 1 mole % both sublattices exhibit activated behaviour over the range of temperatures of Fig.2. Although the motion on the F_2 sublattice apparently does not increase any further, it stays faster than that on F_1. A further discussion of the spin-spin relaxation data is presented in a companion paper, in conjunction with conductivity data [11].

3.2 Spin-lattice relaxation in the rotating frame

The results for $T_{1\rho}$, the spin-lattice relaxation time in the rotating frame, are given in Figs.3-5 for temperatures up to 1050 K. In a proper calculation of the nuclear relaxation in LaF_3 at high temperatures, the dipole-dipole interaction of a moving ^{19}F (I = 1/2) with fluorine on both sublattices, as well as ^{139}La (I = 7/2), have to be taken into account. This was first pointed out by Jaroszkiewicz and Strange [12]. These authors developed a comprehensive theory, which however has not yet been published in detail. Here, we indicate heuristically in which way the dependence of $T_{1\rho}$ on the temperature can be understood.

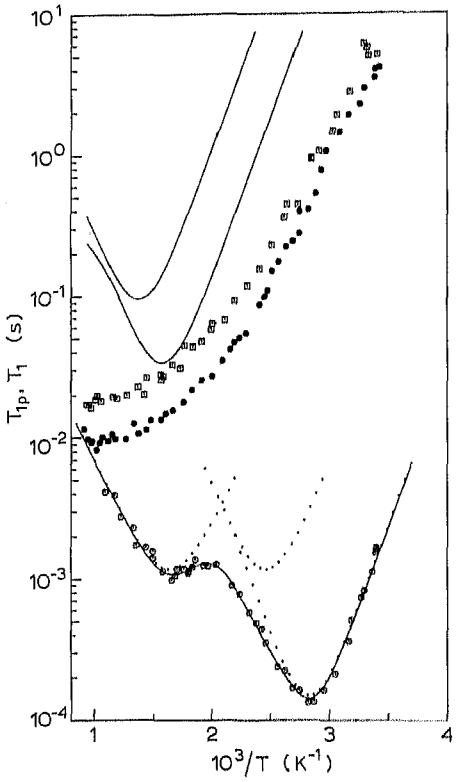

Figure 3 : Spin-lattice relaxation times in pure LaF_3. ⊡ denotes T_1 in the laboratory frame at $\omega_0/2\pi$ = 60.9 MHz, and ● T_1 at 21.5 MHz. ⊙ denotes $T_{1\rho}$ in the rotating frame at a spin-locking field H_1 = 6.2 G. The solid lines represent the results of the calculations. The dotted lines are the three contributions to $T_{1\rho}$.

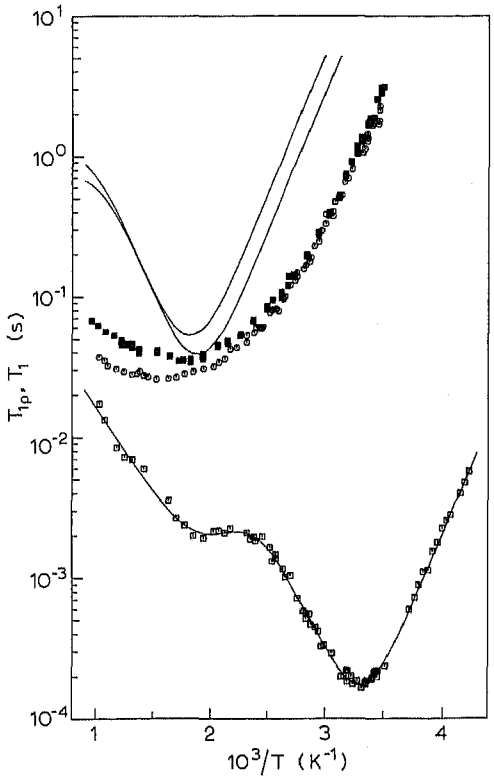

Figure 4 : Same as Fig.3, but LaF_3 doped with 0.3 mole % Ba. ■ denotes T_1 at $\omega_o/2\pi$ = 39.1 MHz, ⏲ T_1 at 28.7 MHz, and ⊡ $T_{1\rho}$ at H_1 = 8.2 G.

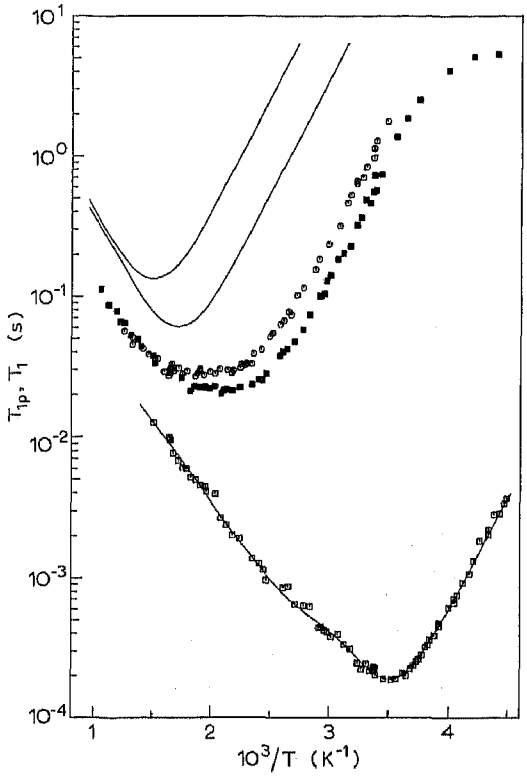

Figure 5 : Same as Fig.3, but LaF_3 doped with 5 mole % Ba. ■ denotes T_1 at $\omega_o/2\pi$ = 28.7 MHz, ⏲ T_1 at 63.2 MHz, and ⊡ $T_{1\rho}$ at H_1 = 6.2 G. The F_2 and F_1 contributions have become substantially less distinct relative to the pure and 0.3 mole % cases.

At low temperatures only the F_2 ions exhibit a fast motion. In this case the nuclear dipole-dipole interactions of the moving fluorine among themselves and with the rigid F_1 sublattice give the major contributions to the relaxation. The spin-lattice relaxation rate in the rotating frame can then be expressed by

$$\frac{1}{T_{1\rho}^{(2)}} = W_{22}\,\frac{\tau_2}{1+4\omega_1^2\tau_2^2} + W_{21}\,\frac{\tau_2}{1+\omega_1^2\tau_2^2}\,, \qquad (1)$$

where τ_2 is the correlation time for hopping within the F_2 sublattice, and $\omega_1 = \gamma H_1$ is the angular precession frequency in the spin-locking field; W_{22} and W_{21} are the rigid-lattice second moments for the F_2 - F_2 and F_2 - F_1 interactions, respectively. Contributions involving $\omega_o = \gamma H_o$ and the F_2 - La interaction are negligible. At very high temperatures the motion within the F_2 sublattice ceases to be effective ($\omega_1\tau_2 \ll 1$), and the dominant relaxation is due to the slower motion on the F_1 sublattice. The corresponding rate is

$$\frac{1}{T_{1\rho}^{(1)}} = W_1\,\frac{\tau_1}{1+\omega_1^2\tau_1^2}\,, \qquad (2)$$

with τ_1 the correlation time within the F_1 sublattice. Intermediate to the regimes where the F_2 and F_1 relaxations are effective, i.e., around 350 and 600 K, respectively, the onset of the F_1 - F_2 exchange gives however rise to a third contribution to the relaxation. Here, $T_{1\rho}$, and for that matter T_2 [2], is determined by a number of mechanisms, such as the transport of magnetization between the sublattices. Effectively, however, the contributions of exchange to the relaxation can be cast in the Bloembergen-Purcell-Pound form. That is,

$$\frac{1}{T_{1\rho}^{(ex)}} = W_{ex} \frac{\tau_{ex}}{1+\omega_1^2\tau_{ex}^2} , \qquad (3)$$

in which τ_{ex} is associated with the hopping between F_1 and F_2 sites. The exchange also modifies W_1 in Eq.(2) from the value the second moment of an undisturbed F_1 sublattice would have. Summarizing, we have

$$\frac{1}{T_{1\rho}} = \frac{1}{T_{1\rho}^{(2)}} + \frac{1}{T_{1\rho}^{(ex)}} + \frac{1}{T_{1\rho}^{(1)}} . \qquad (4)$$

Equation (4) was fitted to the data of pure LaF_3 as well as the Ba-doped systems, with generally excellent results (Figs.3-5). In the adjustment a simple activated behaviour of the correlation times was assumed, i.e., $\tau_i = \tau_i^\infty \exp(\Delta E_i/k_BT)$. The fitted parameters for $La_{1-x}Ba_xF_{3-x}$ with x = 0.3 %, for instance, are for the correlation times $\tau_2^\infty = (6 \pm 1) \times 10^{-13}$ s, $\tau_{ex}^\infty = (4 \pm 2) \times 10^{-10}$ s, and $\tau_1^\infty = (1.7 \pm 0.2) \times 10^{-8}$ s, for the activation energies $\Delta E_2 = 0.40 \pm 0.01$ eV, $\Delta E_{ex} = 0.27 \pm 0.01$ eV, and $\Delta E_1 = 0.25 \pm 0.01$ eV, and for the second moments $W_{22} + W_{21} = (4.8 \pm 0.1) \times 10^9$ rad^2/s^2 and $W_1 = W_{ex} = (1.9 \pm 0.1) \times 10^8$ rad^2/s^2. (The fits do not separate W_{22} and W_{21}, nor distinguish significantly between the output values of W_1 and W_{ex}.) It is noteworthy that the results for $W_{22} + W_{21}$ and W_1 compare well with calculated F_2 - F and F - La second moments, respectively, corroborating the above heuristic approach.

As for the development with the Ba concentration (Figs.3-5), the three contributions become less distinct with increasing x. At 350 K, for instance, the ratio τ_1/τ_2 as obtained from the fitting falls from 160 for x = 0.9 % to 5 for x = 10 %; at 700 K the ratios are about 600 and 50, respectively. For the highly doped samples ($x \geq 5$ %) the exchange part could not be resolved, and in this context it should be noted that the output values of the fitting are to some extent dependent on the model. This does however not affect the general conclusion of convergence of the correlation times on the two sublattices with increasing Ba concentration. The $T_{1\rho}$ data thus confirm the low-temperature T_2 results.

3.3 Spin-lattice relaxation in the laboratory frame

We finally comment on the data for the spin-lattice relaxation time T_1. In the region where $\omega_o\tau >> 1$, the measured T_1's are faster by an order of magnitude than the T_1's calculated on the basis of diffusion alone with the parameters of the $T_{1\rho}$ fits (Figs.3-5). Apparently, T_1 is dominated, also in the pure sample, by impurities including the dopant ions. A second argument for relaxation induced by impurities is found in the anomalously weak dependence on frequency. Thirdly, the activation energy derived from T_1 in the regime $\omega_o\tau >> 1$ turns out to be independent of the Ba concentration ($\Delta E \approx 0.33$ eV), and generally lower than ΔE_2 from $T_{1\rho}$. The T_1 data, unlike those of $T_{1\rho}$ and T_2, do therefore not allow a deduction of the mobilities, despite the long relaxation times T_1 observed in our samples at low temperatures (up to 40 s at 100 K for x = 0.3 %).

Acknowledgements

The work was financially supported by the Netherlands Foundations FOM and ZWO. A. Roos and M. Ouwerkerk are gratefully acknowledged for providing the samples, and J.J. van der Linden and J.L.L.M. Wieman for participating in the construction of the microprocessor system.

REFERENCES

[1] Lee, K. and Sher, A., Phys. Rev. Letters 14 (1965) 1027.
[2] Goldman, M. and Shen, L., Phys. Rev. 144 (1966) 321; Shen, L., Phys. Rev. 172 (1968) 259.
[3] Lundin, A.G. and Gabuda, S.P., Sov. Phys. Solid State 9 (1967) 273.
[4] Ildstad, E., Svare, I. and Fjeldly, T.A., Phys. Stat. Sol. (a) 43 (1977) K65.
[5] Chadwick, A.V., Hope, D.S., Jaroszkiewicz, G. and Strange, J.H., in Fast Ion Transport in Solids (Elsevier, Amsterdam, 1979), p. 683.
[6] Igel, J.R., Wintersgill, M.C., Fontanella, J.J., Chadwick, A.V., Andeen, C.G. and Bean, V.E., J. Phys. C 15 (1982) 7215.
[7] Schoonman, J., Oversluizen, G. and Wapenaar, K.E.D., Solid State Ionics 1 (1980) 211.
[8] Mansmann, M., Z. Anorg. Allg. Chem. 331 (1964) 98.
[9] Sobolev, B.P., Fedorov, P.P., Seiranian, K.B. and Tkachenko, N.L., J. Solid State Chem. 17 (1976) 201.
[10] Roos, A., Mat. Res. Bull., in press.
[11] Roos, A., Aalders, A.F., Schoonman, J., Arts, A.F.M. and de Wijn, H.W., this conference.
[12] Jaroszkiewicz, G.A. and Strange, J.H., J. Physique 7 (1980) C6-246.